⌘ *Author's Choice*

Changes in protein function underlie the disease spectrum in patients with CHIP mutations

Sabrina C. Madrigal[‡1], Zipporah McNeil[‡1], ⑩ Rebekah Sanchez-Hodge[‡], Chang-he Shi[§], Cam Patterson[¶],
⑩ Kenneth Matthew Scaglione[∥], and ⑩ Jonathan C. Schisler[‡**2]

From the [‡]*McAllister Heart Institute, The University of North Carolina at Chapel Hill, Chapel Hill, North Carolina 27599,*
[§]*Department of Neurology, The First Affiliated Hospital of Zhengzhou University, Zhengzhou University, Zhengzhou 450052,
Henan, China,* [¶]*University of Arkansas for Medical Sciences, Little Rock, Arkansas 72205,* [∥]*Department of Molecular Genetics and
Microbiology, Duke University, Durham, North Carolina 27710, and* [**]*Department of Pharmacology and Department of Pathology
and Lab Medicine, The University of North Carolina at Chapel Hill, Chapel Hill, North Carolina 27599*

Edited by George N. DeMartino

Monogenetic disorders that cause cerebellar ataxia are characterized by defects in gait and atrophy of the cerebellum; however, patients often suffer from a spectrum of disease, complicating treatment options. Spinocerebellar ataxia autosomal recessive 16 (SCAR16) is caused by coding mutations in STUB1, a gene that encodes the multifunctional enzyme CHIP (C terminus of HSC70-interacting protein). The disease spectrum of SCAR16 includes a varying age of disease onset, cognitive dysfunction, increased tendon reflex, and hypogonadism. Although SCAR16 mutations span the multiple functional domains of CHIP, it is unclear whether the location of the mutation and the change in the biochemical properties of CHIP contributes to the clinical spectrum of SCAR16. In this study, we examined relationships between the clinical phenotypes of SCAR16 patients and the changes in biophysical, biochemical, and functional properties of the corresponding mutated protein. We found that the severity of ataxia did not correlate with age of onset; however, cognitive dysfunction, increased tendon reflex, and ancestry were able to predict 54% of the variation in ataxia severity. We further identified domain-specific relationships between biochemical changes in CHIP and clinical phenotypes and specific biochemical activities that associate selectively with either increased tendon reflex or cognitive dysfunction, suggesting that specific changes to CHIP–HSC70 dynamics contribute to the clinical spectrum of SCAR16. Finally, linear models of SCAR16 as a function of the biochemical properties of CHIP support the concept that further inhibiting mutant CHIP activity lessens disease severity and may be useful in the design of patient-specific targeted approaches to treat SCAR16.

⌘ *Author's Choice—Final version open access under the terms of the Creative Commons CC-BY license.*
[1] Both authors made equal contributions to this work.
[2] To whom correspondence should be addressed: UNC McAllister Heart Institute, 3340C Medical Biomolecular Research Bldg., 111 Mason Farm Rd., Chapel Hill, NC 27599-7126. Tel.: 919-843-8708; E-mail: schisler@unc.edu.

Ataxia is a general term used to describe a loss of coordination. Ataxia can be caused by a variety of diseases, including metabolic disorders, vitamin deficiencies, peripheral neuropathy, cancer, and brain injuries. In addition to deterioration in movement and balance, ataxia can be accompanied by a spectrum of secondary disorders, including impairments in speech, vision, and cognitive ability. Ataxia is most often caused by the progressive deterioration of the cerebellum, known as cerebellar ataxia (CA),[3] of which there are several causes: hyperthyroidism, alcoholism, stroke, multiple sclerosis, and traumatic injury. Additionally, there are known genetic mutations that are thought to cause CA, and these forms of CA are classified by their inheritance patterns (1). CA mutations are inherited most commonly in an autosomal recessive manner (estimated prevalence is 7 per 100,000). CA can also manifest as an autosomal dominant disorder (estimated prevalence is 3 per 100,000) in addition to less prevalent X-linked or mitochondrial form of inheritance. Most forms of autosomal dominant CAs are caused by polyglutamine expansions within a protein coding region, in contrast to autosomal recessive CAs that are caused by conventional mutations within the coding region (1). The age of onset, prognosis, and accompanying symptoms vary both among and within the genetic forms of CA, and importantly, there are currently no frontline medications for CA (2).

Spinocerebellar ataxia autosomal recessive 16 (SCAR16; MIM 615768) is a recessive form of cerebellar ataxia with a wide-ranging disease spectrum that can also include hypogonadism, cognitive dysfunction, dysarthria, and increased tendon reflex (2). Using whole-exome sequencing, we identified a mutation in *STUB1* in two patients initially diagnosed with ataxia and hypogonadism (3). Subsequently, numerous clinical reports identified *STUB1* mutations in patients with ataxia, confirming our initial identification of a new disease (3–10). Remarkably, *STUB1* mutations were found in nearly 2% of Cau-

---

[3] The abbreviations used are: CA, cerebellar ataxia; SCAR16, spinocerebellar ataxia autosomal recessive 16; CHIP, C terminus of HSC70-interacting protein; HSC70, heat shock cognate 71-kDa protein; STUB1, STIP1 homology and Ubox-containing protein 1; AOO, age of onset; TR, tendon reflex; CD, cognitive dysfunction; SARA, scale for the assessment and rating of ataxia; PLS, partial least squares; HSP, heat shock protein; TPR, tetratricopeptide repeat; Ub, ubiquitin; ANOVA, analysis of variance; VIP, variable importance for the projection; FDR, false discovery rate; CC, coiled-coil.

SASBMB

casian patients with degenerative ataxia, and these mutations appeared to be specific to the ataxia phenotype and not rare ubiquitous polymorphisms (8). *STUB1* encodes the multifunctional enzyme CHIP (C terminus of HSC70-interacting protein), recognized as an active member of the cellular protein quality-control machinery and has multiple functions as both a chaperone (11, 12), cochaperone (13, 14), and ubiquitin ligase enzyme (15, 16). As a chaperone, CHIP can cause structural changes to proteins to either maintain solubility or increase specific activity. As a cochaperone, CHIP directly interacts with heat shock proteins (HSPs) and can aid in the stabilization and refolding of HSP-bound substrates. Conversely, as a ubiquitin ligase, CHIP ubiquitinates terminally defective proteins and targets them for degradation by the ubiquitin–proteasome system.

SCAR16 mutations span the three functional domains of CHIP (Fig. 1*A*): the N-terminal tetratricopeptide repeat (TPR) domain that binds HSPs, the coiled-coiled domain that is important for dimerization, and the C-terminal Ubox domain that is responsible for the ubiquitin ligase function (2). Currently, it is not known whether the location of these mutations mediates specific aspects of the SCAR16 spectrum. Equally so, it is not known how changes in CHIP properties caused by substitution mutations relate to clinical phenotypes. In this report, we combined clinical data provided by numerous reports and a recent report that characterized the biochemical repercussions of several of these SCAR16 disease mutations (see Fig. 1*A*) (17). Our approach allowed us to identify the specific biochemical changes to CHIP that are coupled to SCAR16 clinical characteristics. We developed linear models and used simulations to identify which properties of mutant CHIP proteins may impact disease severity. Defining the relationship between changes in specific features of CHIP and disease phenotypes may both reveal new clues to the spectrum of this disease and, ultimately, guide precision medicine-based strategies to treat SCAR16.

Results

SCAR16 patient demographics and clinical phenotypes

The overall objective of this study was to determine whether biochemical changes in CHIP, caused by disease-associated substitution mutations, correlate to SCAR16 patient phenotypes. The first step in using patient data was to analyze the distribution of and relationship between the clinical variables. A total of eight variables were obtained from clinical reports, including two quantitative variables related to disease severity: *age of onset* (AOO), which refers to when ataxia symptoms were first observed; and scale for the assessment and rating of ataxia (*SARA*), a measure of ataxia severity. In addition, a group of categorical phenotypes can also contribute to the disease spectrum in SCAR16 patients: *increased tendon reflex* (TR), indicative of upper motor neuron dysfunction; *cognitive dysfunction* (CD), the loss of intellectual function; and *hypogonadism*, deficiencies in sex hormone production. Lastly, there were additional qualitative descriptive data from SCAR16 patients that we also considered important in analyzing the disease spectrum, including *sex, ancestry*, and *homozygosity* of the mutation (Table S1; all supporting infor-

Table 1
Patient variables
Abundance for each trait is represented by either the percentage or median (and interquartile range) for categorical or continuous variables, respectively. Super populations for ancestry are as follows: AMR, admixed American; SAS, South Asian; MENA, Middle Eastern/North African; EUR, European; EAS, East Asian. *p* values greater than 0.05 suggest that the variable is normally distributed within the patient cohort.

Trait	Abundance ($n = 24$)	p
Hypogonadism (yes) (%)	17	0.0006
Increased tendon reflex (yes) (%)	75	0.0122
Ancestry (AMR, SAS, MENA, EUR, EAS) (%)	4, 4, 25, 33, 33	0.0126
Cognitive dysfunction (yes) (%)	71	0.0382
AOO (years)	17 (10)	0.0674
SARA (score)	18.5 (16.4)	0.1413
Homozygosity (yes) (%)	46	0.6829
Sex (male) (%)	54	0.6829

mation files cited in text are available at the UNC digital repository, https://doi.org/10.17615/8dqf-e678).

The patient cohort was first summarized by analyzing the distribution of the clinical variables (Table 1). The median AOO was 17 years of age (range = 0.5–49), and the median SARA score was 18.5 (range = 4–40), a value associated with moderate dependence for daily activities (18). There was nearly an equal number of males and females, as well as homozygous and compound heterozygous patients. Most notably, hypogonadism was found in only four patients, whereas over 70% of the patients suffered from increased tendon reflex and/or cognitive dysfunction.

Relationships within the clinical spectrum of SCAR16

To determine whether SCAR16 patients had similar combinations of the disease phenotypes (CD, increased TR, and hypogonadism), we used contingency analysis, a statistical method to measure the relationship between categorical variables. There was no association between any combination of the variables (Table 2), suggesting that these three phenotypes occur independently from one another.

In other forms of spinocerebellar ataxia, younger AOO is linked to increased ataxia severity, and we hypothesized that the same trend would apply to SCAR16. Counter to our hypothesis, there was no correlation between AOO and SARA as measured by linear regression (Fig. 1*B*). However, CHIP plays an important and global role in aging, seen both in rodent models and in some SCAR16 patients with accelerated aging characteristics (10, 19, 20). Hence, there may be additional complexities in regard to the loss of CHIP function and age-dependent phenotypes, such as AOO.

Next, we measured the associations of patient variables with either AOO or SARA (Table S2). The only patient variable that associated with AOO (false discovery rate (FDR) < 10%) was the type of mutation. SCAR16 is a recessive disorder caused by either a homozygous mutation (the same mutation on each allele) or a compound heterozygous mutation (different mutation on each allele). In other recessive forms of spinocerebellar ataxia, homozygous mutations associate with earlier AOO and higher degrees of ataxia (21, 22). The AOO of SCAR16 patients with homozygous mutations was 12 years earlier than patients with compound heterozygous mutations (Fig. 1*C*). However, there was no link between homozygosity and SARA (Table S2),

Table 2

Contingency analysis of SCAR16 disease spectrum

The *p* values of the two-tailed Fisher's exact test in comparing the pairwise occurrence of hypogonadism (HG), increased tendon reflex (TR), and cognitive dysfunction (CD) are shown. *p* values greater than 0.05 suggest that the phenotypes being compared are independent of one another.

Trait	*p*
HG *vs.* CD	0.2833
HG *vs.* TR	0.2513
CD *vs.* TR	1.0000

Figure 2. Multivariable regression model of SARA in SCAR16 patients. *A*, model coefficients and their variable importance in projection values from PLS regression analysis represented by scatter plot. *Y*, yes; *N*, no; *EAS*, East Asian ancestry; *EUR*, European ancestry. The *dotted line* represents the VIP cutoff for inclusion into the final model. *B*, actual SARA *versus* predicted SARA (SARA$_{adj}$) plot of the PLS model of each SCAR16 patient.
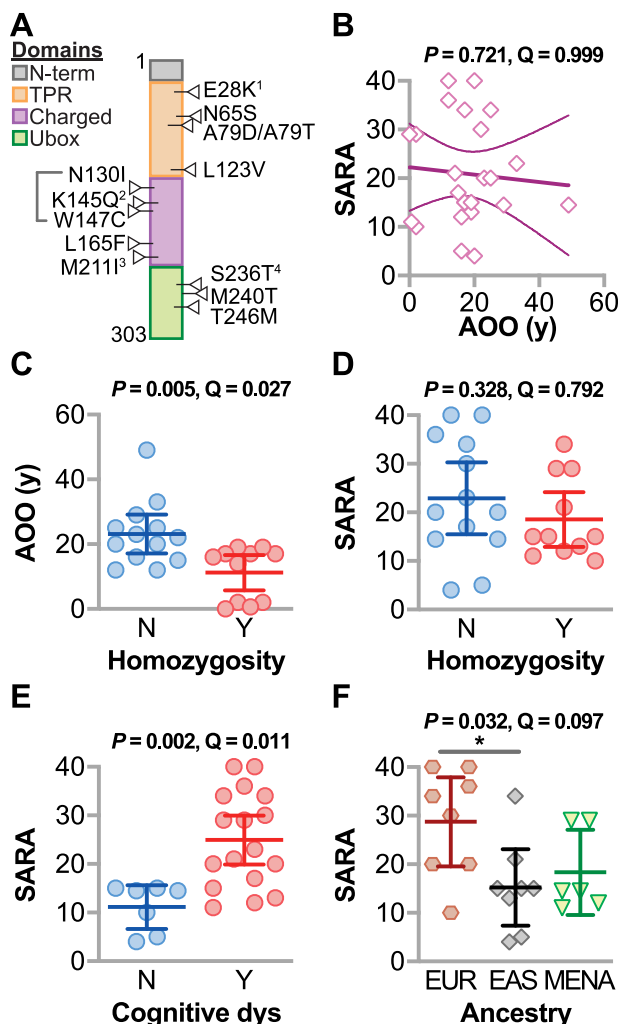

Figure 1. Relationship between SCAR16 clinical variables. *A*, locations of the biochemically characterized SCAR16 mutations across the various functional domains of CHIP. Compound mutations with a second preterminal stop codon allele are indicated: 1K144*, 2Y230Cfx*8, 3E238*, and 4Y207*. *B*, regression analysis of AOO and SARA summarized by the best-fit line and the 95% confidence interval. *C–E*, AOO (*C*) and SARA score (*D*) of SCAR16 patients stratified by homozygosity as well as SARA score (*E*) of SCAR16 patients stratified by cognitive dysfunction (*dys*). Data are represented by dot plot and summarized by the mean ± 95% confidence interval, analyzed by *t* test. *F*, SARA score of SCAR16 patients stratified by ancestry: *EUR*, European; *EAS*, East Asian; *MENA*, Middle Eastern/North African. Data are represented by dot plot and summarized by the mean with *error bars* indicating the 95% confidence interval, analyzed by ANOVA: *, $p < 0.05$ via Tukey post hoc test. The *p* and *Q* values of each analysis are indicated above the panel.

again highlighting the discordance between AOO and SARA in SCAR16 patients (Fig. 1*B*).

We found that SCAR16 patients diagnosed with CD on average had SARA scores 10 points higher than those with normal cognitive skills (Fig. 1*E*). Also, patients with European ancestry
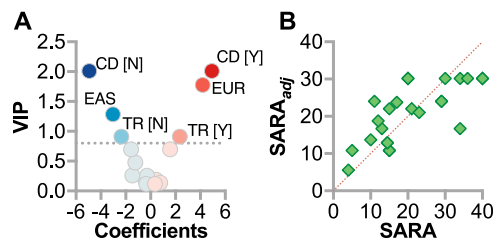
had the highest average SARA (Fig. 1*F*; median = 32), whereas there was no difference between those with Han Chinese or Middle Eastern/North African ancestry (median = 15 and 14.5, respectively). These data demonstrate that SCAR16 patients with CD had more severe deficits in motor function and that other genetic factors may potentially influence the effect of CHIP mutations on the severity of ataxia.

Phenotypes linked to SCAR16 severity

As detailed above, several covariates exist within the patient data, comprising a mixture of quantitative and categorical variables. Multivariate analysis allows us to consider the combined effect of several variables on a given outcome. To determine the impact of multiple patient variables on the severity of ataxia in SCAR16 patients, we used partial least squares (PLS) regression. This modeling technique was selected because it permits the usage of both quantitative and categorical variables; additionally, PLS can be used with correlated variables.

PLS identified three factors, CD, ancestry, and TR (Fig. 2*A*), that together explained 54% of the variation in SARA (Fig. 2*B*). The remaining variables, homozygosity, AOO, and sex, did not improve the predictive power of the modeling. The adjusted SARA score (SARA$_{adj}$) was determined by Equation 1.

$$SARA_{adj} = 17.2 + [5.6(CD_Y), -5.6(CD_N)] + [4.7(EUR), 0.9(SAS),$$

$$-1.4(MENA), -1.7(AMR), -3.4(EAS)]$$

$$+ [2.7(TR_Y), -2.7(TR_N)] \quad \text{(Eq. 1)}$$

where Y = yes, N = no, EUR = European ancestry, SAS = South Asian, MENA = Middle Eastern/North African, AMR = admixed American, and EAS = East Asian ancestry.

In the PLS model, CD had the largest effect on SARA (±5.6 points); increased TR also contributed to SARA (±2.7 points). These findings are consistent with the role of cognition and proper tendon reflexes in assessing the extent of motor dysfunction in patients. Remarkably, our model suggests that even when accounting for CD and TR, genetic factors associated with ancestry may influence the severity of SCAR16, nearly 5 points on the SARA scale.

Changes in CHIP biochemistry caused by SCAR16 mutations

CHIP has three primary domains: 1) multiple TPR domains located in the N-terminal region of CHIP that mediate interactions with HSPs, such as HSP70; a coiled-coil (CC) domain that
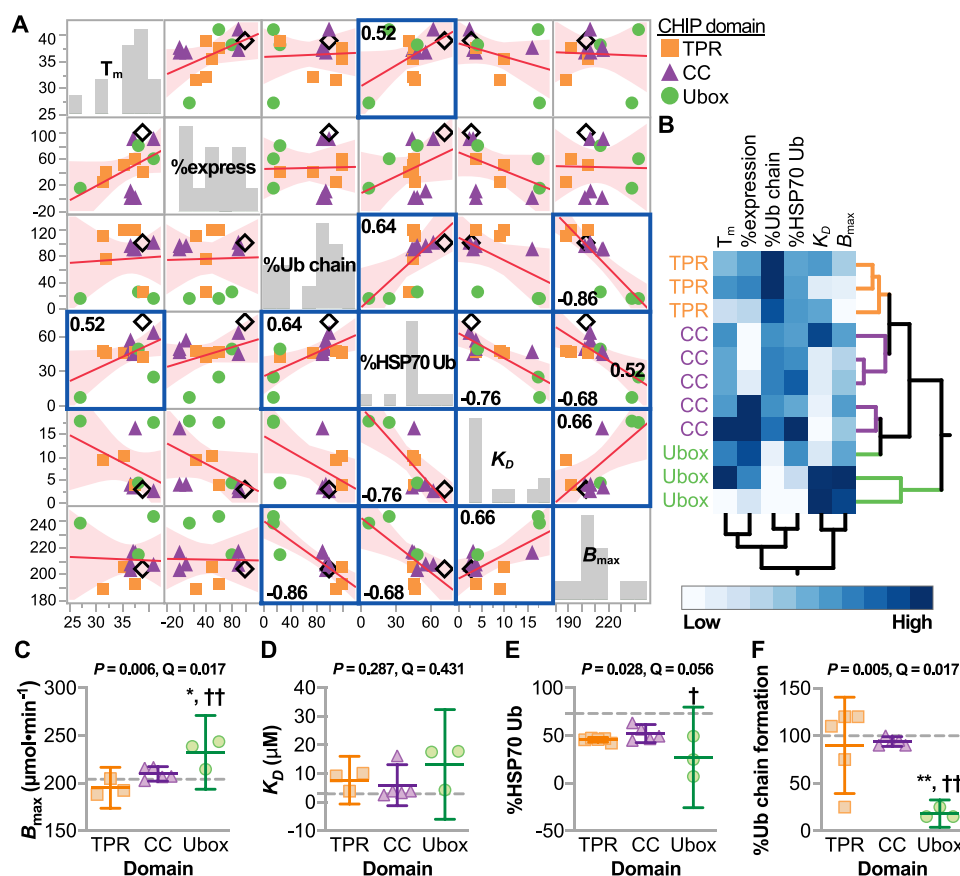
Figure 3. Domain-specific changes in the biochemistry of mutant CHIP proteins. *A*, multivariate correlations of the biochemical properties of mutant CHIP proteins represented by scatter plot and summarized by the best-fit line and the 95% confidence interval; highlighted correlations indicate the Pearson correlation coefficients (ρ) with <10% FDR. *B*, unsupervised hierarchical clustering of the biochemical variables from mutant CHIP proteins identified by the domains harboring the mutation. *C–F*, biochemical variables stratified by the location of the mutation. Data are represented by dot plot and summarized by the mean with *error bars* indicating the 95% confidence interval. The *p* and *Q* values of the ANOVA are indicated above each panel. Tukey post hoc test was used: * and ** indicate $p < 0.05$ and 0.001, respectively, compared with the CC domain; † and †† indicate $p < 0.05$ and 0.001, respectively, compared with the TPR domain. The *dashed lines* indicate levels measured using CHIP-WT protein.

influences dimerization of CHIP; and the Ubox domain, located in the C-terminal region of CHIP, that mediates the transfer of ubiquitin (Ub) to a substrate protein. Synthetic mutations in either the TPR or Ubox domains, K30A and H260Q, abolish interactions with HSPs or the ubiquitin ligase activity of CHIP, respectively, and have been used over the past decade to delineate the multifunctional aspects of CHIP. SCAR16 mutations span all three domains of CHIP, highlighting the potential importance of all three domains in regard to cerebellar function. A recent study analyzed the effect of SCAR16 mutations on the properties of CHIP at the protein level (17); however, the study did not look at how these changes in CHIP biochemistry related to the human disease phenotypes.

Prior to associating changes in CHIP properties with specific SCAR16 phenotypes, we first needed to identify relationships between various biophysical and biochemical properties to better understand the overarching effect of these mutations on CHIP function (Table S3). Data include the binding affinity (K_D) and binding capacity (B_{max}) of CHIP to a peptide containing the EEVD binding motif, found in the C-terminal tail of HSP70. The EEVD motif is the recognition sequence for proteins with TPR domains, such as CHIP. Functionality of the Ubox was measured by two parameters. Proper ubiquitin ligase activity requires the ligase to interact both with Ub-conjugating

proteins, known as E2 enzymes, and the substrate that is ubiquitinated. Decreases in ubiquitin chain formation between CHIP and the E2 enzyme can identify defects in E2 recruitment, independent of CHIP–substrate interactions. This ubiquitin chain formation represents one measure of Ubox function (%Chain). The second measurement of Ubox function was the ubiquitination of full-length HSP70 (%HSP70 Ub), requiring intact E2–CHIP–substrate interactions. Intrinsic effects of the SCAR16 mutations on CHIP properties included the thermostability of recombinant protein (melting temperature (T_m)), the oligomeric form of CHIP protein, and the relative protein stability of CHIP when introduced into a human cell line (%E).

All continuous data were normally distributed except for K_D, which did not meet normalcy testing even after various transformations; therefore, all analyses were conducted using nontransformed data to identify correlations (Fig. 3A). Multiplicity was controlled for all pairwise tests by using an FDR cutoff of <10% (Table S4). There was a strong positive correlation between E2-dependent ubiquitin chain formation (17) and the extent of HSP70 ubiquitination ($\rho = 0.64$). This was expected, given that E2-dependent ubiquitin chain formation is required for efficient ubiquitination of the substrate protein, in this case HSP70. Also, HSP70 ubiquitination was inversely correlated with the K_D between CHIP and a peptide containing the

Biochemical and clinical modeling of SCAR16

HSP70-binding motif ($\rho = -0.76$). We observed a positive correlation between B_{max} and K_D regarding CHIP interactions with the HSP70 peptide ($\rho = 0.66$). This unexpected positive correlation suggests that some mutant CHIP proteins, including CHIP-T246M, may have an increased binding capacity toward chaperones, consistent with our previous studies (3, 19). Mutant CHIP proteins appeared to group based on the domain that harbors the mutation in the scatter plots (Fig. 3A). This observation was confirmed via hierarchical clustering of mutant CHIP proteins and their corresponding biochemical parameters. Mutant proteins clustered primarily by the domain harboring the mutation (Fig. 3B), supporting the premise that the domain affected by the mutation may have differential actions on CHIP activities.

The relationship between the location of the mutation affecting specific activities was confirmed via ANOVA and was driven predominantly by Ubox mutations. Three associations were measured at an FDR <10% (Table S5). First, Ubox mutations had increased binding capacity toward HSP70 (Fig. 3C); however, there was no difference in binding affinity (Fig. 3D), suggesting that additional, nonspecific interactions may result from Ubox mutations. Second, all mutant CHIP proteins maintained some capacity to polyubiquitinate HSP70 except for two Ubox mutants, M240T and T246M (Fig. 3E). Third, all Ubox mutants had a reduced capacity to form polyubiquitin chains, perhaps due to altered interactions with E2 enzymes, whereas TPR and CC mutations were not defective in these same conditions (Fig. 3F). These data suggest that Ubox mutations, in particular, affect functions that span both the cochaperone and ubiquitin ligase functions of CHIP.

The link between protein biochemistry and patient phenotypes caused by SCAR16 mutations

Finally, to explore the biochemical mechanisms of how CHIP mutations contribute to SCAR16, we combined the clinical phenotypic data from patients with the corresponding biochemical characteristics of mutant CHIP proteins. This approach has limitations. First, only substitution mutations were characterized biochemically; therefore, frameshift mutations are not included in this analysis. Second, given the recessive and sometimes compound heterozygous nature of SCAR16, these analyses were performed on a per allele basis. However, the majority of the compound heterozygous mutations include one mutation with a preterminal stop codon, predicted to be degraded by nonsense-mediated RNA decay (Table S1). Hypogonadism was reported in only three patients and was not included in these analyses.

Ubox mutations are linked to cognitive dysfunction

There was no link found between the domain harboring the mutation and the continuous variables AOO, SARA, or SARA$_{adj}$, as measured by ANOVA ($p = 0.51$, 0.86, or 0.14, respectively). However, in analysis of the categorical disease phenotypes, there was a highly skewed distribution between the mutation location and cognitive dysfunction (Fig. 4). Most notably, 94% of alleles with Ubox mutations associated with cognitive dysfunction. In contrast, there was no difference in the frequency of cognitive dysfunction between TPR
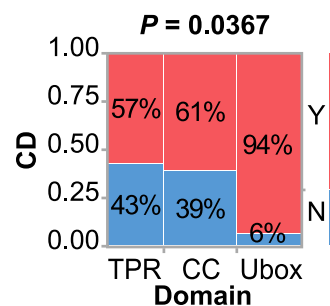

Figure 4. Ubox mutations are linked to a higher incidence of cognitive dysfunction. Shown is the contingency analysis of the location of disease alleles and the presence of CD in SCAR16 patients, analyzed using Fisher's exact test. The percentages of mutated alleles with or without CD within each domain are indicated. *Y*, yes; *N*, no.

or CC allele mutations (59% of TPR or CC alleles associated with cognitive dysfunction). In contrast, increased TR was equally distributed across the domains of CHIP (Fisher's exact test = 1.00). These data suggest that domain-specific changes in CHIP function may contribute to the clinical spectrum of SCAR16, particularly Ubox mutations that are linked with cognitive dysfunction.

Biochemical changes caused by SCAR16 mutations associate with cognitive dysfunction and increased tendon reflex

One of our primary goals of this study was to determine whether specific changes to CHIP biochemistry are related to the disease spectrum in SCAR16 patients. We used associative statistical tests to identify relationships using two disease phenotypes of SCAR16 (increased TR and CD) and the biochemical changes in CHIP using an FDR cutoff of <10% (Table S6). T_m and %E of mutant CHIP proteins did not associate with either CD ($p = 0.57$ and 0.58) or increased TR ($p = 0.28$ or 0.62). However, there was a 35% decrease in ubiquitin chain formation linked to CD alleles (Fig. 5A), suggesting that this activity is essential to maintain cerebellar cognition. CHIP functions primarily as a dimer, and seven of the 13 characterized mutations maintained a dimeric distribution similar to CHIP-WT, whereas a subset of mutant CHIP proteins formed higher-order oligomers (17). Interestingly, dimeric forms of mutant CHIP associated with increased TR (Fig. 5B). Thus, the loss of Ubox function may be a prominent contributor to impaired cognition, whereas mutant forms of CHIP that still form dimers, and perhaps some degree of altered CHIP function, may be involved in the pathology related to increased tendon reflex.

This dichotomy between cognitive and reflex phenotypes extended to the remaining biochemical data. Several variables changed reciprocally when compared with either cognitive dysfunction or tendon reflex. Cognitive dysfunction–linked mutations had higher B_{max} (Fig. 5C) with no change in K_D (Fig. 5D). In contrast, tendon reflex mutations associated with lower B_{max} (Fig. 5E) and lower K_D (Fig. 5F), at levels comparable with the binding characteristics of CHIP-WT. Although only reaching marginal significance, opposite effects on HSP70 ubiquitination were observed with cognitive dysfunction and tendon reflex mutations (Fig. 5, G and H). Differential biochemical activities of CHIP linked with CD and TR support the concept that altered CHIP–HSP70 dynamics, caused by disease mutations, may contribute to the clinical spectrum of SCAR16.
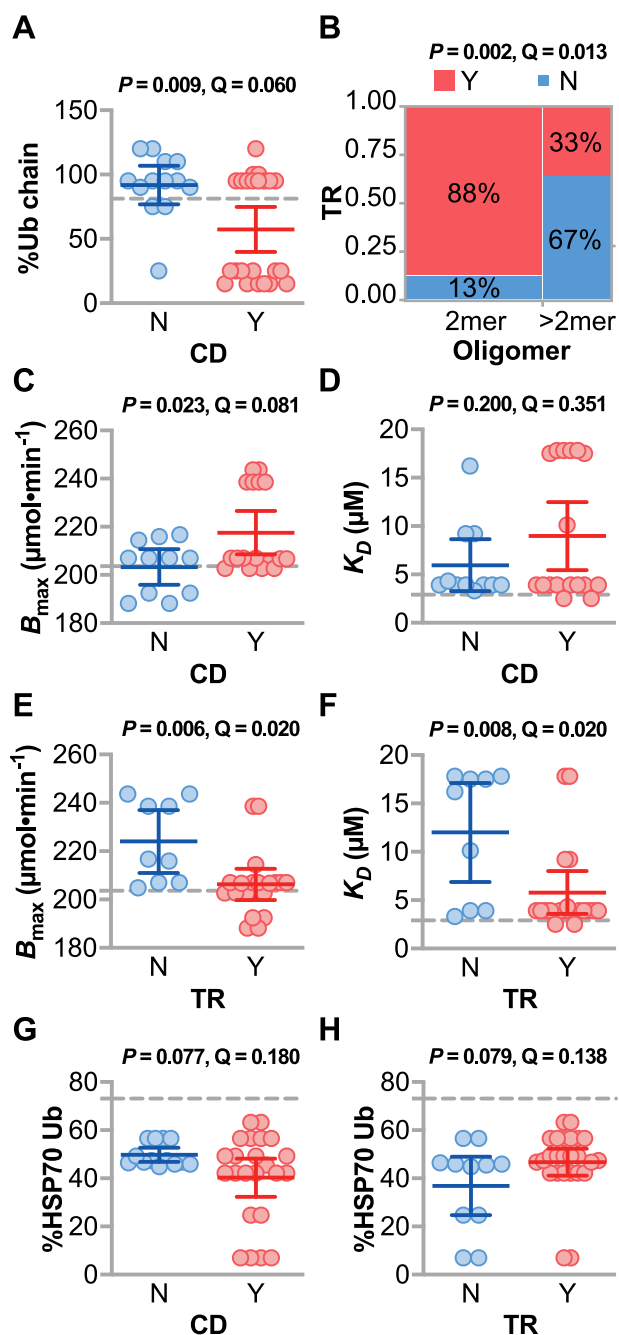
Figure 5. Changes in the biochemical properties of mutant CHIP proteins associate with clinical features of SCAR16. *A*, the amount of ubiquitin chain formation (*%Ub chain*) of mutant CHIP proteins relative to CHIP-WT stratified by the presence of CD found in SCAR16 patients. Data are represented by dot plot and summarized by the mean ± 95% confidence interval, analyzed by *t* test. The *dashed line* indicates the activity in WT CHIP. *B*, contingency analysis of the oligomerization pattern of mutant CHIP proteins and the presence of increased TR in SCAR16 patients, analyzed using Fisher's exact test. The percentages of mutated alleles with or without increased TR within each domain are indicated. *C–H*, the indicated biochemical variables of mutant CHIP proteins stratified by either the presence of CD or increased TR found in SCAR16 patients. Data are represented by dot plot and summarized by the mean with *error bars* indicating the 95% confidence interval, analyzed by *t* test. The *dashed line* indicates the activity of WT CHIP. The *p* and *Q* values of each analysis is indicated above the panel. *Y*, yes; *N*, no.

Biochemical modeling of AOO and SARA in SCAR16

We used the same linear model approach, used above in describing the patient phenotypes, to understand the changes

in CHIP biochemistry that may contribute to both AOO and SARA. First, bivariate analysis (FDR < 10%) found that CHIP proteins with decreased ubiquitin chain formation and higher B_{max} were associated with an earlier AOO (Table S7). Additionally, either CHIP proteins that form higher-order oligomers or those with reduced binding affinities associated with lower SARA scores. These data suggest that nonfunctional forms of CHIP (higher-order oligomers and decreased HSC70 binding affinity) result in less severe ataxia, as opposed to mutant CHIP proteins that still maintain normal tertiary structure and binding activities toward chaperones. To determine the *combination* of biochemical changes to CHIP that would predict less severe disease outcomes, we used PLS modeling and simulations to identify the multiple changes in CHIP biochemistry that would result in both delaying AOO and decreasing SARA. A PLS model of both AOO and SARA was generated using HSP70 ubiquitination, E2-dependent ubiquitin chain formation, K_D, and B_{max}.

$$AOO_{adj} = 20.6 - 3.9\left[\frac{(\%HSP70ub - 43.7)}{15.5}\right]$$

$$+ 5.3\left[\frac{(\%Chain\ formation - 69.9)}{39.0}\right] + 4.9\left[\frac{(K_D - 7.8)}{6.0}\right]$$

$$- 7.1\left[\frac{(B_{max} - 212.0)}{16.6}\right] \quad (Eq.\ 2)$$

$$SARA_{adj2} = 18.8 + 1.9\left[\frac{(\%HSP70ub - 43.7)}{15.5}\right]$$

$$+ 0.2\left[\frac{(\%Chain\ formation - 69.9)}{39.0}\right] - 2.3\left[\frac{(K_D - 7.8)}{6.0}\right]$$

$$+ 0.3\left[\frac{(B_{max} - 212.0)}{16.6}\right] \quad (Eq.\ 3)$$

The initial modeling and simulations with biochemical variables from patient data resulted in an average AOO and SARA of 20.6 and 18.8, respectively (Fig. S1; actual = 17.7 and 20.9). Next, we asked how would the biochemical parameters change to see a predicted decrease in disease severity? To do this, we set our improvement target to be one standard deviation away from the mean, equating to an 11-year increase in AOO and a 10-point decrease in SARA. We then ran simulations to identify the changes in CHIP biochemistry that would best reach these improvement targets. The results of the simulation were consistent regarding AOO and SARA: further inhibiting mutant CHIP activity toward HSP70, either by decreasing HSP70 ubiquitination and/or reducing the binding affinity to HSP70, predicts both a delay in AOO (Fig. 6A) and decreased SARA (Fig. 6B). Specifically, the simulations found that a delay in the age of onset by 7.2 years and an 8.2-point decrease in SARA were predicted when the affinity of mutant CHIP proteins to HSP70 was reduced to 17 μM and HSP70 ubiquitination was decreased to 7.2% relative to WT CHIP (Table 3). Thus, further inhibiting mutant CHIP activities may be a useful approach to lessen the severity of SCAR16.
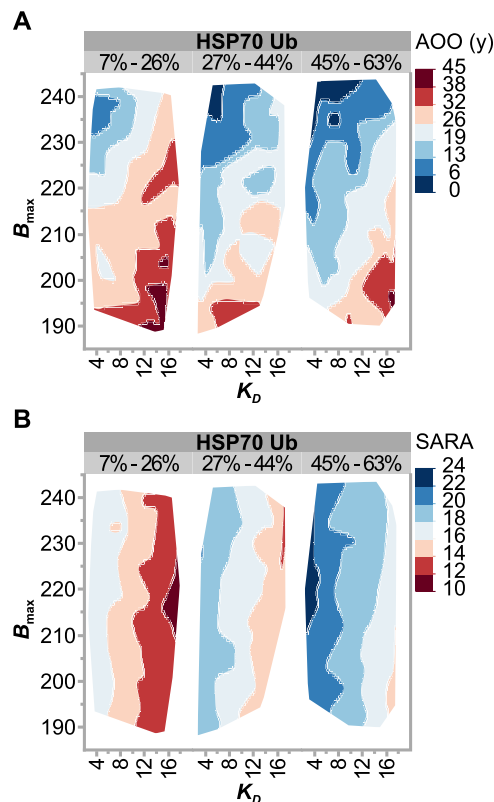
SASBMB

J. Biol. Chem. (2019) 294(50) 19236–19245 **19241**

Figure 6. Simulation results of CHIP biochemical properties that improve disease phenotypes. *A* and *B*, simulation results of AOO (A) and SARA (B), represented as contour plots of B_{max} as a function of K_D, grouped by the percentage of HSP70 ubiquitination relative to WT CHIP. Each outcome variable (AOO and SARA) is represented by color range, *red* to *blue*, corresponding to less to more severe disease conditions.

Table 3

Monte Carlo simulations of AOO and SARA in SCAR16 using biochemical properties of CHIP

The values of HSP70 ubiquitination (%HSP70 Ub) and ubiquitin chain formation (%Ub chain), equilibrium dissociation constant (K_D; μM), and amount of HSP70 binding (B_{max}; μmol·min^{-1}) for WT CHIP are provided. The results of the simulating AOO and SARA using the experimental biochemical data of mutant CHIP proteins (SCAR16) compared with the model optimized to reduce disease severity (SCAR16$_{opt}$) are indicated. N/A, not applicable.

	%HSP70 Ub	%Ub chain	K_D	B_{max}	AOO	SARA
WT CHIP	73.1	100	2.9	204	N/A	N/A
Simulation						
SCAR16	44	70	7.8	212	20.6	18.8
SCAR16$_{opt}$	7.2	15	17	217	27.8	10.6

Discussion

Mutations that cause SCAR16 span the three functional domains of the multifunctional enzyme CHIP (Fig. 1*A*). Prior to this study, it was not known whether the location of these mutations associates with specific aspects of the clinical spectrum exhibited by SCAR16 patients. Equally so, it was not known how changes in CHIP properties, caused by substitution mutations, related to clinical phenotypes.

Initially, we found that, in addition to cognitive dysfunction and increased tendon reflex, genetic background may influence the severity of SCAR16 (Figs. 1, *E* and *F*, and 2*A* and Table S3). It is possible that quality and access to health care and environmental factors could confound the observation of ancestry on

SCAR16 severity; however, there could be other genetic factors that could lessen or exacerbate the loss or change in CHIP function. Identifying genetic modifiers of CHIP function may provide additional therapeutic opportunities to treat SCAR16 and related spinocerebellar ataxias.

Ultimately, we were interested in identifying the patterns of mutation-specific effects on CHIP function and how these changes in CHIP biochemistry contribute to the clinical spectrum of SCAR16 phenotypes. Overall, we found two primary groupings of mutations. First, Ubox mutations had a more dramatic effect on the overall loss of CHIP function (Fig. 3) and strongly associated with cognitive dysfunction in SCAR16 patients (Figs. 4 and 5). Second, in contrast, mutations with more modest effects on CHIP function, primarily the mutations located in the TPR and CC domains, were linked to the increased tendon reflex seen in SCAR16 patients (Fig. 5). Therefore, mutations that retain this intact, but slightly diminished activity toward HSP70, appear to drive the increased tendon reflex pathology.

These data allowed us to generate linear models to identify properties of CHIP that may be useful to target in SCAR16 patients. Our simulation results were consistent with the idea that inhibiting mutant CHIP interactions with HSP70 predict a later AOO and less severe ataxia (Fig. 6 and Table 3). As expected, there was a strong negative correlation between the amount of HSP70 ubiquitination and K_D of the CHIP–HSP70 interaction (Fig. 3*A*; $\rho = -0.76$), suggesting that blocking the CHIP–HSP interaction represents a therapeutic opportunity that can be explored in future studies.

It remains unclear why Ubox mutations, with disrupted ubiquitin-related activities, strongly associate with cognitive dysfunction. Ubox mutations also have higher B_{max}, and we previously observed that the Ubox mutant CHIP-T246M pulled down more HSC70 and HSP70 compared with WT CHIP in both cell models and in our engineered mouse line that expresses CHIP-T246M from the endogenous locus (3, 19). One possibility is that Ubox mutants still bind E2 enzymes, but the inability to transfer ubiquitin disrupts E2 function and perhaps activity of E2 enzymes toward other E3 ligases. Alternatively, the propensity to form higher-order oligomers (17, 19) and changes in solubility (19) could also affect the function of proteins that still interact with Ubox mutants. Overall, our data suggest that inhibiting the interaction between mutant CHIP and HSP70 chaperones could be used as a targeted approach in cognitively normal patients with TPR and CC domain mutations. In contrast, SCAR16 patients with cognitive dysfunction and Ubox mutations may benefit from the use of molecular chaperones to prevent the oligomerization of these mutant CHIP proteins. CHIP impacts several cellular pathways, and identifying the CHIP-dependent pathways that may contribute to the specific pathologies in SCAR16, such as necroptosis (23), IGF1 (24), mitophagy (25), autophagy (26, 27), or water balance (28), may also uncover therapeutically relevant targets. Additionally, gene therapy approaches might be applicable to SCAR16. The obvious solution is to use gene editing approaches to correct these mutations; however, given the recessive nature of the disease, delivery of a functional copy of CHIP may also be beneficial (29, 30); alternatively, antisense oligonu-

cleotide therapy that can down-regulate mutant CHIP protein levels may also prove to be an effective approach (31).

Additional SCAR16 patients with new, uncharacterized mutations continue to be reported (9, 32–35), in addition to a possible variant that functions in a dominant manner (36). With additional clinical data and the advent of new molecular, cellular, and preclinical models to study CHIP function, it is likely that precision-based approaches could be developed based on the specific mutation or the specific loss of function. Finally, by looking more broadly at the various autosomal recessive ataxias, additional themes and targets that could be effective across multiple ataxia diseases may also come to light in the years to come (37).

Experimental procedures

SCAR16 patient data

Clinical data were obtained from published reports (Table S1) (3–10). One measure of disease severity is the score from SARA. When SARA scores were not implicitly stated, SARA was imputed based on the clinical report (18).

CHIP mutation data

All biophysical and biochemical properties of CHIP proteins with disease-associated substitution mutations were obtained from published data (Table S2) (17). HSP70 ubiquitination was measured by densitometry analysis and represented by the total amount of HSP70 that was modified by ubiquitination; WT CHIP ubiquitinated 73 or 81% of the total HSP70 in the reaction, respectively.

Statistical computations

All analyses were performed using JMP Pro (v14.2.0) as detailed below.

Distribution analysis

Continuous and categorical clinical variable distributions were analyzed using the Shapiro–Wilk W test or likelihood ratio χ^2 test, respectively. Probabilities less than 0.05 reject the null hypothesis that the variables are from either a normal or even distribution.

Significance testing and multiplicity

The null hypothesis of an individual statistical test was rejected when $p < 0.05$. In cases where there were multiple factors tested simultaneously against a response, a multiple test correction was used to control false positives at an FDR of <10%. The Benjamini–Hochberg Q value (FDR-adjusted p value) was calculated for dependent variable associations or across all pairwise comparisons, in either bivariate or multivariate analyses, respectively, as described below. Both the raw p values and Q values are reported. Post hoc tests, when applicable, are described in the figure legends.

Bivariate analysis

Bivariate analysis was performed using either t test or ANOVA (comparing continuous to categorical variables), linear regression (comparing two continuous variables), or contingency analysis using Fisher's exact test (comparing two cat-

egorical variables). The p value is the result of testing the null hypothesis that there is no association between the variables.

Multivariate analysis

The Pearson product-moment correlation coefficient was used to measure the strength of the linear relationships between each pair of response variables. An exact linear relationship between two variables has a correlation of 1 or −1, depending on whether the variables are positively or negatively related. The correlation tends toward zero as the strength of relationship decreases. The p value is the result of testing the null hypothesis that the correlation between the variables is zero.

Hierarchical clustering

Variables were standardized and clustered using Ward's minimum variance method where the distance between clusters is the sum of squares between the two clusters summed over all the variables.

Regression analysis

Partial least squares regression was initially performed using all variables, using leave-one-out cross-validation. The variable importance for the projection (VIP) statistic was determined for each initial variable. The VIP is a weighted sum of squares of the weights, and the higher the VIP score, the more influential a variable is in the regression model. Variables with VIP values >0.8 were retained in the final equation (38, 39).

Simulations

Monte Carlo simulations were performed by modeling SARA and AOO using a multiple y partial least squares regression equation with the indicated variables (38–41). Targets for SARA and AOO improvement were set at one standard deviation from the mean. Simulations were run using all x variables as random with a normal distribution. 5000 baseline simulations were used to fit the original data. The simulation was adjusted to maximize desirability via an additional 5000 simulations to identify parameters that maximize improvement of both y variables (42).

Data availability

All extracted data were handled. Table S1 contains the clinical variables. Table S2 contains the bivariate analysis summary of SARA and AOO with SCAR16 patient phenotypes. Table S3 contains the biochemical data. Table S4 contains the multivariate analysis summary of CHIP biochemical properties. Table S5 contains the analysis summary of SCAR16 mutation locations with the biochemical properties of the encoded mutant CHIP proteins. Table S6 contains the analysis summary of either cognitive dysfunction or increased tendon reflex with the biochemical properties of CHIP. Table S7 contains the analysis summary of either SARA or AOO associations with each biochemical property of CHIP. Fig. S1 displays the regression model of AOO and SARA as a function of the biochemical properties of CHIP. All supporting information files are available at the UNC digital repository, https://doi.org/10.17615/8dqf-e678.

References

1. Bird, T. D. (1993) Hereditary Ataxia Overview, in *GeneReviews®* (Adam, M. P., Ardinger, H. H., Pagon, R. A., Wallace, S. E., Bean, L. J., Stephens, K., and Amemiya, A., eds) University of Washington, Seattle, WA http://www.ncbi.nlm.nih.gov/books/NBK1138/ (accessed March 29, 2019)

2. Ronnebaum, S. M., Patterson, C., and Schisler, J. C. (2014) Emerging evidence of coding mutations in the ubiquitin–proteasome system associated with cerebellar ataxias. *Hum. Genome Var.* **1,** 14018 CrossRef Medline

3. Shi, C.-H., Schisler, J. C., Rubel, C. E., Tan, S., Song, B., McDonough, H., Xu, L., Portbury, A. L., Mao, C.-Y., True, C., Wang, R.-H., Wang, Q.-Z., Sun, S.-L., Seminara, S. B., Patterson, C., *et al.* (2014) Ataxia and hypogonadism caused by the loss of ubiquitin ligase activity of the U box protein CHIP. *Hum. Mol. Genet.* **23,** 1013–1024 CrossRef Medline

4. Shi, Y., Wang, J., Li, J.-D., Ren, H., Guan, W., He, M., Yan, W., Zhou, Y., Hu, Z., Zhang, J., Xiao, J., Su, Z., Dai, M., Wang, J., Jiang, H., *et al.* (2013) Identification of CHIP as a novel causative gene for autosomal recessive cerebellar ataxia. *PLoS One* **8,** e81884 CrossRef Medline

5. Bettencourt, C., de Yébenes, J. G., López-Sendón, J. L., Shomroni, O., Zhang, X., Qian, S.-B., Bakker, I. M., Heetveld, S., Ros, R., Quintáns, B., Sobrido, M.-J., Bevova, M. R., Jain, S., Bugiani, M., Heutink, P., *et al.* (2015) Clinical and neuropathological features of spastic ataxia in a Spanish family with novel compound heterozygous mutations in STUB1. *Cerebellum* **14,** 378–381 CrossRef Medline

6. Cordoba, M., Rodriguez-Quiroga, S., Gatto, E. M., Alurralde, A., and Kauffman, M. A. (2014) Ataxia plus myoclonus in a 23-year-old patient due to STUB1 mutations. *Neurology* **83,** 287–288 CrossRef Medline

7. Depondt, C., Donatello, S., Simonis, N., Rai, M., van Heurck, R., Abramowicz, M., D'Hooghe, M., and Pandolfo, M. (2014) Autosomal recessive cerebellar ataxia of adult onset due to STUB1 mutations. *Neurology* **82,** 1749–1750 CrossRef Medline

8. Synofzik, M., Schüle, R., Schulze, M., Gburek-Augustat, J., Schweizer, R., Schirmacher, A., Krägeloh-Mann, I., Gonzalez, M., Young, P., Züchner, S., Schöls, L., and Bauer, P. (2014) Phenotype and frequency of STUB1 mutations: next-generation screenings in Caucasian ataxia and spastic paraplegia cohorts. *Orphanet J. Rare Dis.* **9,** 57 CrossRef Medline

9. Hayer, S. N., Deconinck, T., Bender, B., Smets, K., Züchner, S., Reich, S., Schöls, L., Schüle, R., De Jonghe, P., Baets, J., and Synofzik, M. (2017) STUB1/CHIP mutations cause Gordon Holmes syndrome as part of a widespread multisystemic neurodegeneration: evidence from four novel mutations. *Orphanet J. Rare Dis.* **12,** 31 CrossRef Medline

10. Heimdal, K., Sanchez-Guixé, M., Aukrust, I., Bollerslev, J., Bruland, O., Jablonski, G. E., Erichsen, A. K., Gude, E., Koht, J. A., Erdal, S., Fiserstrand, T., Haukanes, B. I., Boman, H., Bjørkhaug, L., Tallaksen, C. M., *et al.* (2014) STUB1 mutations in autosomal recessive ataxias—evidence for mutation-specific clinical heterogeneity. *Orphanet J. Rare Dis.* **9,** 146 CrossRef Medline

11. Rosser, M. F., Washburn, E., Muchowski, P. J., Patterson, C., and Cyr, D. M. (2007) Chaperone functions of the E3 ubiquitin ligase CHIP. *J. Biol. Chem.* **282,** 22267–22277 CrossRef Medline

12. Schisler, J. C., Rubel, C. E., Zhang, C., Lockyer, P., Cyr, D. M., and Patterson, C. (2013) CHIP protects against cardiac pressure overload through regulation of AMPK. *J. Clin. Investig.* **123,** 3588–3599 CrossRef Medline

13. Ballinger, C. A., Connell, P., Wu, Y., Hu, Z., Thompson, L. J., Yin, L.-Y., and Patterson, C. (1999) Identification of CHIP, a novel tetratricopeptide repeat-containing protein that interacts with heat shock proteins and negatively regulates chaperone functions. *Mol. Cell. Biol.* **19,** 4535–4545 CrossRef Medline

14. Dai, Q., Zhang, C., Wu, Y., McDonough, H., Whaley, R. A., Godfrey, V., Li, H.-H., Madamanchi, N., Xu, W., Neckers, L., Cyr, D., and Patterson, C. (2003) CHIP activates HSF1 and confers protection against apoptosis and cellular stress. *EMBO J.* **22,** 5446–5458 CrossRef Medline

15. Jiang, J., Ballinger, C. A., Wu, Y., Dai, Q., Cyr, D. M., Höhfeld, J., and Patterson, C. (2001) CHIP is a U-box-dependent E3 ubiquitin ligase: identification of Hsc70 as a target for ubiquitylation. *J. Biol. Chem.* **276,** 42938–42944 CrossRef Medline

16. Meacham, G. C., Patterson, C., Zhang, W., Younger, J. M., and Cyr, D. M. (2001) The Hsc70 co-chaperone CHIP targets immature CFTR for proteasomal degradation. *Nat. Cell Biol.* **3,** 100–105 CrossRef Medline

17. Kanack, A. J., Newsom, O. J., and Scaglione, K. M. (2018) Most mutations that cause spinocerebellar ataxia autosomal recessive type 16 (SCAR16) destabilize the protein quality-control E3 ligase CHIP. *J. Biol. Chem.* **293,** 2735–2743 CrossRef Medline

18. Schmitz-Hübsch, T., du Montcel, S. T., Baliko, L., Berciano, J., Boesch, S., Depondt, C., Giunti, P., Globas, C., Infante, J., Kang, J.-S., Kremer, B., Mariotti, C., Melegh, B., Pandolfo, M., Rakowicz, M., *et al.* (2006) Scale for the assessment and rating of ataxia: development of a new clinical scale. *Neurology* **66,** 1717–1720 CrossRef Medline

19. Shi, C. H., Rubel, C., Soss, S. E., Sanchez-Hodge, R., Zhang, S., Madrigal, S. C., Ravi, S., McDonough, H., Page, R. C., Chazin, W. J., Patterson, C., Mao, C. Y., Willis, M. S., Luo, H.-Y., Li, Y. S., *et al.* (2018) Disrupted structure and aberrant function of CHIP mediates the loss of motor and cognitive function in preclinical models of SCAR16. *PLoS Genet.* **14,** e1007664 CrossRef Medline

20. Min, J.-N., Whaley, R. A., Sharpless, N. E., Lockyer, P., Portbury, A. L., and Patterson, C. (2008) CHIP deficiency decreases longevity, with accelerated aging phenotypes accompanied by altered protein quality control. *Mol. Cell. Biol.* **28,** 4018–4025 CrossRef Medline

21. Soga, K., Ishikawa, K., Furuya, T., Iida, T., Yamada, T., Ando, N., Ota, K., Kanno-Okada, H., Tanaka, S., Shintaku, M., Eishi, Y., Mizusawa, H., and Yokota, T. (2017) Gene dosage effect in spinocerebellar ataxia type 6 homozygotes: a clinical and neuropathological study. *J. Neurol. Sci.* **373,** 321–328 CrossRef Medline

22. Shang, X.-J., Xu, H.-L., Yang, J.-S., Chen, P.-P., Lin, M.-T., Qian, M.-Z., Lin, H.-X., Chen, X.-P., Chen, Y.-C., Jiang, B., Chen, Y.-J., Chen, W.-J., Wang, N., Zhou, Z.-M., and Gan, S.-R. (2018) Homozygote of spinocerebellar ataxia type 3 correlating with severe phenotype based on analyses of clinical features. *J. Neurol. Sci.* **390,** 111–114 CrossRef Medline

23. Seo, J., Lee, E.-W., Sung, H., Seong, D., Dondelinger, Y., Shin, J., Jeong, M., Lee, H.-K., Kim, J.-H., Han, S. Y., Lee, C., Seong, J. K., Vandenabeele, P., and Song, J. (2016) CHIP controls necroptosis through ubiquitylation- and lysosome-dependent degradation of RIPK3. *Nat. Cell Biol.* **18,** 291–302 CrossRef Medline

24. Tawo, R., Pokrzywa, W., Kevei, É., Akyuz, M. E., Balaji, V., Adrian, S., Höhfeld, J., and Hoppe, T. (2017) The ubiquitin ligase CHIP integrates proteostasis and aging by regulation of insulin receptor turnover. *Cell* **169,** 470–482.e13 CrossRef Medline

25. Lizama, B. N., Palubinsky, A. M., Raveendran, V. A., Moore, A. M., Federspiel, J. D., Codreanu, S. G., Liebler, D. C., and McLaughlin, B. (2018) Neuronal preconditioning requires the mitophagic activity of C-terminus of HSC70-interacting protein. *J. Neurosci.* **38,** 6825–6840 CrossRef Medline

26. Ravi, S., Parry, T. L., Willis, M. S., Lockyer, P., Patterson, C., Bain, J. R., Stevens, R. D., Ilkayeva, O. R., Newgard, C. B., and Schisler, J. C. (2018) Adverse effects of fenofibrate in mice deficient in the protein quality control regulator, CHIP. *J. Cardiovasc Dev. Dis.* **5,** E43 CrossRef Medline

27. Guo, D., Ying, Z., Wang, H., Chen, D., Gao, F., Ren, H., and Wang, G. (2015) Regulation of autophagic flux by CHIP. *Neurosci. Bull.* **31,** 469–479 CrossRef Medline

28. Wu, Q., Moeller, H. B., Stevens, D. A., Sanchez-Hodge, R., Childers, G., Kortenoeven, M. L. A., Cheng, L., Rosenbaek, L. L., Rubel, C., Patterson,

C., Pisitkun, T., Schisler, J. C., and Fenton, R. A. (2018) CHIP regulates aquaporin-2 quality control and body water homeostasis. *J. Am. Soc. Nephrol.* **29,** 936–948 CrossRef Medline

29. Chandler, R. J., Williams, I. M., Gibson, A. L., Davidson, C. D., Incao, A. A., Hubbard, B. T., Porter, F. D., Pavan, W. J., and Venditti, C. P. (2017) Systemic AAV9 gene therapy improves the lifespan of mice with Niemann-Pick disease, type C1. *Hum. Mol. Genet.* **26,** 52–64 CrossRef Medline

30. Cabral-Miranda, F., Nicoloso-Simões, E., Adão-Novaes, J., Chiodo, V., Hauswirth, W. W., Linden, R., Chiarini, L. B., and Petrs-Silva, H. (2017) rAAV8-733-mediated gene transfer of CHIP/Stub-1 prevents hippocampal neuronal death in experimental brain ischemia. *Mol. Ther.* **25,** 392–400 CrossRef Medline

31. Scoles, D. R., Meera, P., Schneider, M. D., Paul, S., Dansithong, W., Figueroa, K. P., Hung, G., Rigo, F., Bennett, C. F., Otis, T. S., and Pulst, S. M. (2017) Antisense oligonucleotide therapy for spinocerebellar ataxia type 2. *Nature* **544,** 362–366 CrossRef Medline

32. Gazulla, J., Izquierdo-Alvarez, S., Sierra-Martínez, E., Marta-Moreno, M. E., and Alvarez, S. (2018) Inaugural cognitive decline, late disease onset and novel STUB1 variants in SCAR16. *Neurol. Sci.* **39,** 2231–2233 CrossRef Medline

33. Turkgenc, B., Sanlidag, B., Eker, A., Giray, A., Kutuk, O., Yakicier, C., Tolun, A., and Temel, S. G. (2018) STUB1 polyadenylation signal variant AACAAA does not affect polyadenylation but decreases STUB1 translation causing SCAR16. *Hum. Mutat.* **39,** 1344–1348 CrossRef Medline

34. García, A. M., Abrevaya, S., Kozono, G., Cordero, I. G., Córdoba, M., Kauffman, M. A., Pautassi, R., Muñoz, E., Sedeño, L., and Ibáñez, A. (2017) The cerebellum and embodied semantics: evidence from a case of genetic ataxia due to STUB1 mutations. *J. Med. Genet.* **54,** 114–124 CrossRef Medline

35. Kawarai, T., Miyamoto, R., Shimatani, Y., Orlacchio, A., and Kaji, R. (2016) Choreoathetosis, dystonia, and myoclonus in 3 siblings with autosomal recessive spinocerebellar ataxia type 16. *JAMA Neurol.* **73,** 888–890 CrossRef Medline

36. Genis, D., Ortega-Cubero, S., San Nicolás, H., Corral, J., Gardenyes, J., de Jorge, L., López, E., Campos, B., Lorenzo, E., Tonda, R., Beltran, S., Negre, M., Obón, M., Beltran, B., Fàbregas, L., *et al.* (2018) Heterozygous STUB1 mutation causes familial ataxia with cognitive affective syndrome (SCA48). *Neurology* **91,** e1988–e1998 CrossRef Medline

37. Synofzik, M., Puccio, H., Mochel, F., and Schöls, L. (2019) Autosomal recessive cerebellar ataxias: paving the way toward targeted molecular therapies. *Neuron* **101,** 560–583 CrossRef Medline

38. Garthwaite, P. H. (1994) An interpretation of partial least squares. *J. Am. Stat. Assoc.* **89,** 122–127 CrossRef

39. Cox, I., and Gaudard, M. (2013) *Discovering Partial Least Squares with JMP,* SAS Institute, Cary, NC

40. Wold, S., Sjöström, M., and Eriksson, L. (2001) PLS-regression: a basic tool of chemometrics. *Chemometr. Intell. Lab. Syst.* **58,** 109–130 CrossRef

41. Eriksson, L., Byrne, T., Johansson, E., Trygg, J., and Vikström, C. (2013) *Multi- and Megavariate Data Analysis Basic Principles and Applications,* Umetrics Academy, Umeå, Sweden

42. Derringer, G., and Suich, R. (1980) Simultaneous optimization of several response variables. *J. Quality Technol.* **12,** 214–219 CrossRef